CLASSIFICATION OF CORNEL ARCUS USING TEXTURE FEATURES WITH BAYESIAN REGULATION BACK PROPAGATION

R. A. Ramlee[1*], A.R. Ramli[2], M. Hanafi[3],
S. Mashohor[4], Z. Mohd Noh[5]

[1,2,3,4]Faculty of Engineering, Communications and Network Engineering, Universiti Putra Malaysia, 43400 UPM, Serdang, Selangor, Malaysia.
[5]Faculty of Electronic and Computer Engineering, Universiti Teknikal Malaysia Melaka, 76100, Melaka, Malaysia.

ABSTRACT

The corneal arcus (CA) is an eye problem frequently faced by some group of people. The CA signs indicate the presence of abnormal lipid in blood and can cause several problems such as blood pressure, diabetes, and hyperlipidemia. This paper presents a comparison of classification of the abnormal eye using a neural network. In order to extract the image features, the gray level co-occurrence matrix (GLCM)was used. This matrix measures the texture of the image, where the statistical calculation can be used to present the image features. The Bayesian Regulation (BR) algorithm has been proposed, in which this classifier classifies the obtained results better than previous works by other researchers. In this experiment, two classes data-set of the eye image, normal and abnormal images CA are used. The results from this BR classifier demonstrate a sensitivity of 96.1 % and a specificity of 98.6 %. The overall accuracy of this proposed system is 97.6 %. Although this classifier does not obtain 100 % accuracy, however its result is proven to be able to classify the CA images successfully.

KEYWORDS: *Corneal arcus; Bayesian regulation; neural network (NN); classifiers; confusion matrix; accuracy.*

1.0 INTRODUCTION

The formation of lipid around the iris is the result of abnormalities caused by excessive levels of lipids present in the blood. Because the eye also contains the blood vessels, this lipid formation can occur in that area. This condition is known as corneal arcus (CA).

CA presence is normal for most people over the age of 50 years. Conversely, for young people such as youth and children who suffer from this condition, they have to undergo a blood test to ensure the level of lipids in their blood. Urbano (2001) stated that CA is normal for older people. This statement is also supported by Chua, Mitchell, Wang (2002) and Urbano (2001), who suggested that cardio heart diseases (CHD) as easy to attack male patients aged below 40 with CA signs. However, for the younger group, CA is said to be related to lipid abnormalities and has high risk for getting CHD. The area where CA frequently appears is around the iris-limbus, with thickness of 0.3 to 1 mm (Chua et al., 2002).

* Corresponding Email : ridza@utem.edu.my

The researchers (Fernández et al., 2007; Hickey et al., 1970; Ang et al., 2011; Cooke, 1981; Bersohn et al., 1969; Chen et al., 2009; Halfon et al., 1984; Pomerantz, 1962; Navoyan, 2003) have studied about CA, where some of them agreed that the presence of CA is manifested with the abnormal lipids in the human circulatory system.

According to Fernández et al.(2007), corneal arcus is associated to coronary heart disease, blood pressure, hypercholesterolemia (Macchiaiolo et al. 2014), xanthelasma, alcohol, cigarette smoking, diabetes (Bansal et al. 2015; Lesmana et al. 2011), and age. Based on this, the presence of CA that is detected during clinical eye examination can be used as an indicator that there is lipid increase in the blood. Furthermore, the usage of CA is useful as a screening method that is non-invasive and painless.

In this section, several studies related to the automatic diagnosis system to detect abnormalities of the cornea, which have been done by some researchers (Hussein et al. 2013; Lesmana et al. 2011; Wibawa & Purnomo 2006; Acharya et al. 2007; Acharya, U et al. 2006; S.V. Mahesh Kumar 2016) are stated. Hussein et al. (2013) evaluated the potential of iridology that is used to diagnose kidney diseases using the wavelet analysis and neural network. Lesmana et al. (2011) studied diabetes mellitus by detecting the abnormalities in pancreatic beta-cells using iris images. Another work detection of diabetes mellitus is presented by Wibawa & Purnomo (2006). Yuan et al. (2014), used the iris intestinal loop texture information for analysis of the gastrointestinal problem. Six texture measures from the grey-level co-occurrence matrix (GLCM) were used to support vector machine (SVM) classification. Nor'aini & Rohilah (2013) studied the vagina and pelvis region, from the iridology chart based on the iris images. The principal component analysis (PCA) and SVM were used for this study. several research studies that have been done for detecting the corneal arcus using image processing referring to iris region and observation of cornea surface are also found.

Acharya et al. (2006) developed the automatic identification graphic user interface for detection of the eye abnormalities. The fuzzy k-means was used in order to extract the features from the eye images. These features are fed to the radial basis function network (RBFN) for training and testing. About 150 subjects (patients)who suffer from CA, glaucoma, and cataract were classed as having an abnormal eye, while others are having normal eyes. This proposed system obtained a specificity of 100 %, a sensitivity of 90 %, and the overall accuracy is 95 %. In another work by Acharya et al. (2006), a comparison between three types of the classification techniques for classifying the abnormalities of the eye was demonstrated. These classifiers are artificial neural network, fuzzy classifier and neuro-fuzzy classifier. A total of 135 subjects were used for the classification of eye diseases. These results produced more than 85 % for sensitivity and specificity was 100 %.

Mahesh Kumar (2016) also discussed the same problem related to CA. The SVM was used for diagnosing CA. Statistical features such as mean, standard deviation, entropy, skewness and kurtosis were used. The proposed method using OTSU threshold has been explained by Ramlee & Ranjit (2009), for detecting CA. The work conducted a study based on the threshold values which represent normal and abnormal eyes. This system has disadvantages since when a different image intensity is used with variation in brightness, the threshold will be affected.

Based on the findings of studies conducted by various researchers (Chua et al., 2002; Urbano, 2001; Fernández et al., 2007; Hickey et al., 1970; Ang et al., 2011; Cooke, 1981; Bersohn et al., 1969; Chen et al., 2009; Halfon et al., 1984; Pomerantz , 1962; Navoyan, 2003), whom found that there is a correlation between corneal arcus and hyperlipidemia. Therefore, these problems can be studied from the point of establishing a system to classify from the normal people.

In this paper, a classification of normal and abnormal images CA is presented using the BR classifier. The BR classification algorithm is proposed based on the results shown which are quite good compared to the method previously conducted by other researchers.

2.0 METHODOLOGY

The proposed framework for this classification process is shown in Figure 1. Based on the above diagram, this framework consists of four stages. The first stage is the input image, consisting of normal eye image and the eye image with CA. The second stage is to extract image features using GLCM. The third stage is BR neural network to train and test the data-set. This neural network (NN) system consists of three cluster nodes: the input, hidden and output. The final stage is to decide whether the eye images belong to normal or abnormal categories.

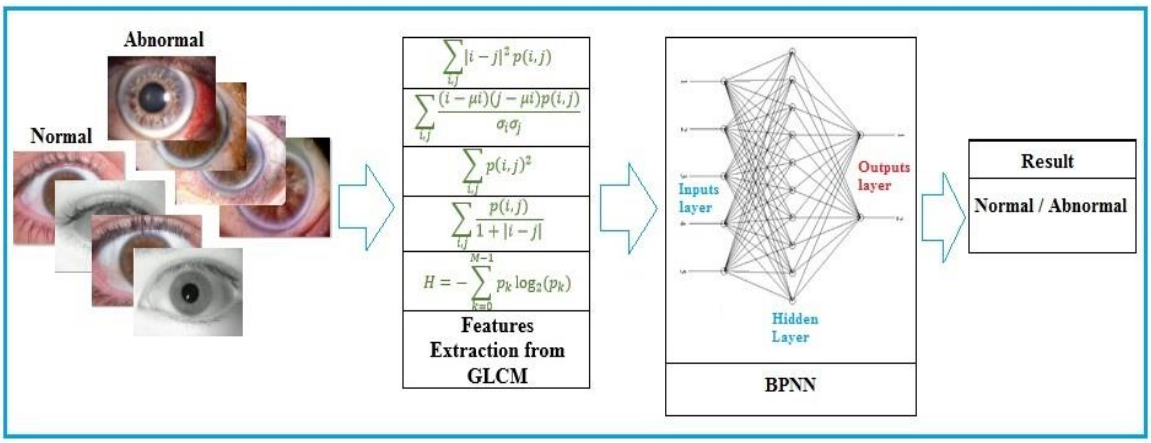

Figure 1. The framework for the proposed methodology

2.1 Database

For this experiment, two sets of data set samples were prepared, which are the normal and abnormal eyes. The data set of the abnormal eyes contains 50 samples while the data set of the normal eyes contains 75 samples. The normal samples are obtained from UBARIS (Proenc & Alexandre, 2006), CASIA (CASIA, 2003), and IITD (Kumar, 2008). Meanwhile, for CA eye, the images were collected from public resources (Andrew Lee, 2005; Harleen et al., 2014; Keepyourhearthealthy, 2010; James, 2002) and other medical and iridology websites. Acharya et al. (2007) collected 50 samples while 135 samples were used by Acharya et al. (2006). Mahesh Kumar (2016) used 100 images acquired from both eyes of 50 patients as a base for their confusion matrix.

2.2 Statistical Features

For feature extraction from the analyzed images, the GLCM matrix was used as suggested by Haralick et al. (1973) where at least 14 textural features are proposed which can be extracted from this GLCM matrix.

In this study, only five of the fourteen statistical texture features are used, in which these minimum features can reduce operating algorithm. The equation of these statistical features is given as follows:

The contrast (f_1) and the local variation can be obtained by calculating the GLCM matrix of Equation 1:

$$f_1 = \sum_{i,j} |i-j|^2 \, p(i,j) \tag{1}$$

The correlation (f_2) measures the amount of joint probability occurrence of the specified pixel pairs in these images.

$$f_2 = \sum_{i,j} \frac{(i-\mu i)(j-\mu i)p(i,j)}{\sigma_i \sigma_j} \tag{2}$$

The energy (f_3) provides the amount of squared elements contained in the GLCM matrix, also known as the angular second moment or uniformity.

$$f_3 = \sum_{i,j} p(i,j)^2 \tag{3}$$

The homogeneity (f_4) measures the nearness of the distribution of components in the GLCM to the GLCM diagonal.

$$f_4 = \sum_{i,j} \frac{p(i,j)}{1+|i-j|} \tag{4}$$

The entropy (f_5) was introduced by Shannon (1948). In the image processing, the entropy is used to calculate the statistical attributes to determine the image texture.

$$f_5 = -\sum_{k=0}^{M-1} p_k \log_2(p_k) \tag{5}$$

The μ is the GLCM mean as given by Equation (6) where P_{ij} is the element in *i* and *j* with normalized symmetrical value contained in the GLCM matrix. *M* is the number of gray levels in the image.

$$\mu = -\sum_{i,j=0}^{M-1} iP_{ij} \tag{6}$$

Meanwhile, σ^2 is the variance of the intensities of all reference pixels in GLCM, as in Equation (7):

$$\sigma^2 = \sum_{i,j=0}^{N-1} P_{ij}\,(i-\mu)^2 \tag{7}$$

2.3 Bayesian Regulation Back-Propagation Algorithm

The over-fitting problems often interfere in the training process of the neural network. For this reason, Foresee & Hagan (1997) implemented BR within the framework of the Levenberg-Marquardt algorithm to solve this problem. Yue et al. (2011) described the regularized training objective function, which is denoted as $F(\omega)$ as written in Equation (8).

$$F(\omega) = \alpha E_\omega + \beta E_D \tag{8}$$

The α and β as in Equation (8), are the parameters of the objective function, while E_ω and E_D are the network weights and network sum error respectively. In BR framework, the network weights are defined as the random variables. These weights of network and training set are assumed as the Gaussian distribution. The factors α and β, are obtained from Bayes' theorem. Equation (9) shows the variables *A* and *B* which are defined from Bayes' theorem that describe posterior and prior probability variables (Li & Shi, 2012).

$$P(A|B) = \frac{P(B|A)P(A)}{P(B)} \tag{9}$$

Referring to Equation (9), the P(A|B) is the conditional of A and B of posterior probability and conversely for P(B|A). Meanwhile, the P(A) and P(B) is the prior of probability of event A and event B. Equation (10) is used to minimize the $F(\omega)$ from Equation (8), in order to optimize the weight space. The variables α and β in Equation (10) are the factors that need to be optimized.

$$P(\alpha,\beta|D,M) = \frac{P(D|\alpha,B,M)P(\alpha,\beta|M)}{P(D|M)} \tag{10}$$

Referring to Equation (10), variable *D* is the distribution of weight, while the *M* is the architecture of NN. Thus, $P(D|M)$ is the factor of normalization. The P(α, $\beta \mid M$) is the regularization parameters and $P(D \mid \alpha, B, M)$ is the function likelihood of *D* with respect to α, *B*, *M*.

The BR is used as shown in Figure 2 for classification of the normal eye and the abnormal eye. A two-layer-feed-forward network, with log-Sigmoid-transfer function at hidden layer and Soft max transfer function at output neurons, are used in this BR. After several

tests, it was decided to use 10 neurons for each training. This NN is designed using five input neurons, ten hidden neurons, and two output neurons. The input to the neural network is derived from the image extraction features. These features include contrast, correlation, energy and the homogeneity and entropy. The images used for this neural network are divided into three sets of data: training data, validation data, and test data.

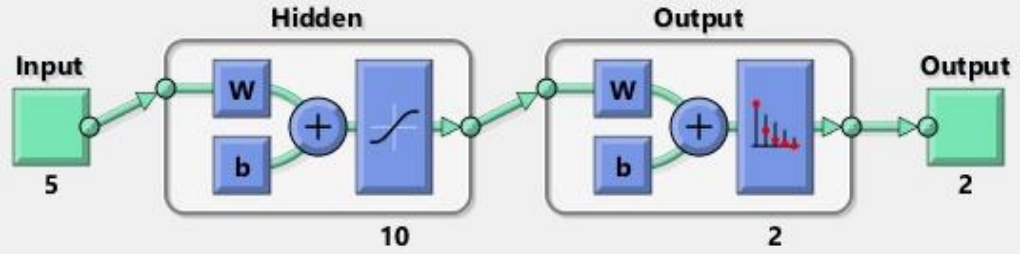

Figure 2 The two layers architecture of the BR

2.4 Evaluation of Classifier Performance

To evaluate the output performance of this model, the confusion matrix (Table 1) and the statistical calculation from the confusion matrix attributes were used. From these attributes, some statistical figures for showing the algorithm performance such as the specificity, sensitivity, and accuracy can be calculated.

Congalton (1991) called the confusion matrix as error matrix or contingency table. The author demonstrated the usage of this error matrix for the classification system, the sampling scheme, the sample size, spatial autocorrelation, and the assessment techniques.

In the confusion matrix, there are four different situations to represent the data. The elements of true-positive (TP) in Table 1 represent the number of samples of correct classification based on the classifier as a positive (abnormal eye).

Table 1. The confusion matrix distribution elements

	Reference	
Predicted	Class I	Class II
Class I	TP	FP
Class II	FN	TN

TP=True positive, FP=False positive, FN=False negative, TN=True negative

Meanwhile, the elements of true-negative (TN) represent the number of samples in the classified correctly by the classifier as a negative (normal eye). The confusion matrix will gain 100% accuracy if both TP and TN detect correctly for each class.

The sensitivity *(Se)* is a measure of the positive elements that are correctly identified by the algorithm (e.g. the percentage of the eye samples which are correctly identified as having the condition of the disease). The sensitivity calculation is given by Equation (11).

$$Se = TPR = \frac{TP}{P} = \frac{TP}{TP + FN} \tag{11}$$

The specificity (*Sp*) is a measure of the percentage of the negative rate, which is opposite to sensitivity (e.g. the percentage of the eye samples which are correctly identified as not having the disease) and given by:

$$Sp = \frac{TN}{N} = \frac{TN}{FP + TN} \tag{12}$$

The accuracy *(ACC)* is a measure of the positive and negative classes that are correctly identified by the algorithm. The calculation is given by Equation (13).

$$ACC = \frac{TP + TN}{P + N} \tag{13}$$

According to Powers (2007), the precision *(PPV)* refers to the proportion of the predicted positive cases that are correctly real positives.

$$PPV = \frac{TP}{TP + FP} \tag{14}$$

3.0 RESULTS AND DISCUSSION

This section presents the results obtained from the experiments conducted and discussion on the classifier performance. Figure 3 shows the receiver operating characteristic (ROC) graph used to present the performance of this classifier system. Two classes are used to classify the eye images, which are the Class 1 and Class 2 for normal eye (controlled) and abnormal eye, respectively. The data of the true positive rate (TPR) against the false positive rate (FPR) are plotted and shown in Figure 3. The percentage of positive predictive value (PPV) is 98 %, and the negative predictive value (NPV) is 97.33 %.

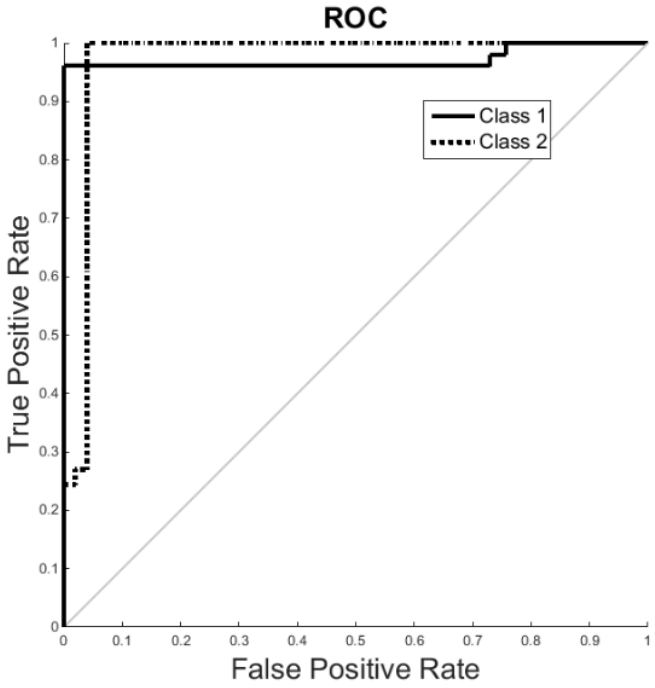

Figure 3. Receiver operating characteristic for BR.

Table 2 presents the comparison between the different methods used to classify the abnormal eye. The highlighted and bold font refer to a proposed system using BR classifier which shows the improvement of overall accuracy achieved.

Table 2. Comparison of method used to classify the abnormal eye

Method	**Se (%)**	**Sp (%)**	**Ppv (%)**	**Npv (%)**	**Acc (%)**
ANN (Acharya, U et al. 2006)	85.00	100	100	80.00	90.74
RBF (Acharya et al. 2007)	90.00	100	100	91.00	95.00
FUZZY (Acharya, U et al. 2006)	89.00	100	100	83.33	92.73
ANFIS (Acharya, U et al. 2006)	89.0	100	100	83.33	92.73
SVM (S.V. Mahesh Kumar 2016)	94.00	98.00	97.91	94.23	96.00
Proposed BR	**96.10**	**98.60**	**98.00**	**97.33**	**96.70**

Se = sensitivity, Sp = specificity, Ppv = positive predictive value, Npv = negative predictive value, Acc = Accuracy.

Table 3 shows the statistical analysis using Kruskal-Wallis (KW) ANOVA table for all features proposed in this experiment. It can be observed that the statistical features of the normal and abnormal eye consist of different data sets. The *P*-values in the last column of Table 3 are compared to the Chi-square values for showing the features that are significant or not. From this table, all texture features indicated reject the null hypothesis that the features come from the same distribution at a 5 % significance level.

Table 3. Kruskal-Wallis ANOVA Table

Features	Source	SS	df	MS	Chi-sq	*P*>Chi-sq
1	Columns	6377.7826	1	6377.7826	8.9451	2.7822E-3
	Error	58504.7174	90	650.0524		
	Total	64882.5	91			
2	Columns	2739.1739	1	2739.1739	3.8418	4.999E-02
	Error	62143.3261	90	690.4814		
	Total	64882.5	91			
3	Columns	18624.8	1	18624.8	26.12	3.205E-07
	Error	46257.2	90	514		
	Total	64882	91			
4	Columns	12029.3913	1	12029.391	16.872	4.00E-05
	Error	52853.1087	90	587.2568		
	Total	64882.5	91			
5	Columns	3669.1413	1	3669.1413	5.1589	2.3128E-2
	Error	61052.3587	90	678.3595		
	Total	64721.5	91			

P =probability

The evaluation of this BR using confusion matrix is shown in Figure 4 where this binary classification is used to get the classification outcome, either positive or negative result. This 2-by-2 matrix comprises of C (m, n), where m and n are the row and column, respectively. For example, in Figure 4, the C (1, 1) for training confusion matrix is represented by the value of 44 samples of the images.

This equals to 41.5 % of the image detected as a correct class. Other statistical values that can be obtained from this training confusion matrix are: accuracy (98.1 %), sensitivity (95.7 %), and specificity (100 %). For test data, this classifier obtained the following values, TP (26.3 %), TN (68.4 %), FP (5.3 %), and FN (0 %). Thus, this classifier demonstrated the results (test data) as follow: the accuracy (94.7 %), sensitivity (100 %), and specificity (92.9 %). The overall results obtained from this BR classifier are given by these values: the accuracy (97.6 %), sensitivity (96.1 %), and specificity (98.6 %).

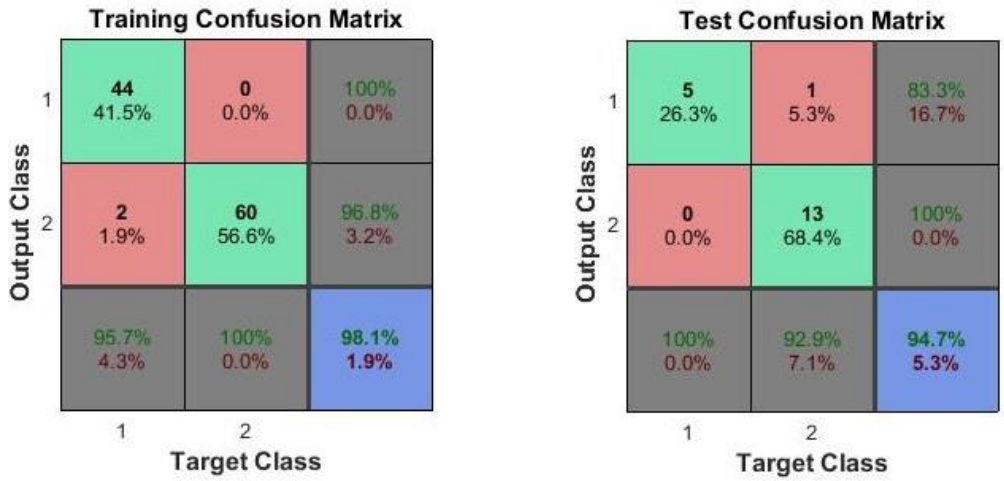

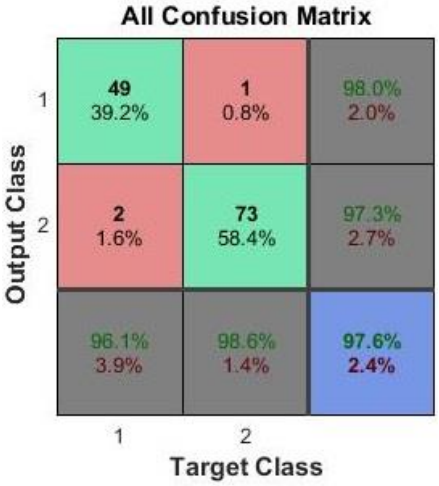

Figure 4. Confusion matrix for BR

4.0 CONCLUSION

In this paper, the classification of CA images using the BR classifier is presented. The image features are extracted using the GLCM matrix properties as the inputs to the BR classifier. These image features are divided by the ratio of 70% for training, 15% for testing, and 15% for validation for the process of classification. Two layers BR model is used for these processes of learning, training, and validation. The network is designed with five inputs, ten hidden neurons, and two output neurons, where this classifier demonstrates a great performance of the classification accuracy (96.7%). Based on these experiments, the accuracy of this algorithm is considered is influenced by the quality of the image, number of images, and the image features used as input classifier. It is proposed that future work should consider other types of eye diseases and identify the best way to get the image characteristics used in the neural network.

ACKNOWLEDGEMENTS

The authors would like to thank Universiti Putra Malaysia and all its staff who have contributed their ideas and supportive materials to prepare this paper until submission. The authors also wish to thank Universiti Teknikal Melaka Malaysia and Kementerian Pengajian Tinggi Malaysia, which provide guidance, support, and sponsorship for this study.

REFERENCES

Acharya, U.R., Kannathal N., Ng, E. Y. K., Min, L.C, & Suri, J. S. (2006). *Computer-based classification of eye diseases*. Engineering in Medicine and Biology Society. IEEE, 1, 6121–4.

Acharya, U.R., Wong, L.Y., Ng, E.Y.K. & Suri, J.S. (2007). Automatic identification of anterior segment eye abnormality. ITBM-RBM, 28, 35–41.

Andrew Lee, M., (2005). *MedicalEye. Department of Ophthalmology at the University of Iowa.* Retrieved from http://webeye.ophth.uiowa.edu/eyeforum/atlas/pages/Arcus/index.htm.

Ang, M., Wong, W., Park, J., Wu, R. Lavanya, R., Zheng, Y., Cajucom-Uy, H., Tai, E.S. & Wong T.Y. (2011). Corneal arcus is a sign of cardiovascular disease, even in low-risk persons. *American Journal of Ophthalmology*, 152(5), 864–871.e1.

Bansal, A., Agarwal, R. & Sharma, R.K. (2015). Determining diabetes using iris recognition system. *International Journal of Diabetes in Developing Countries*, 35(4), 432–438.

Bersohn, I., Politzer, W.M. & Blumsohn, D. (1969). Arcus senilis corneae, its relationship to serum lipids in the South African Bantu. *South African Medical Journal*, 43(33), 1025–1027.

CASIA, (2003). *CASIA iris image database collected by Institute of Automation, Chinese Academy of Sciences.* Retrieved from http://www.sinobiometrics.com.

Chen, H.T., Chen, H.C., Hsiao, C.H., Ma, D.H Chen, Y.T. & Lin K.K. (2009). Corneal arcus and cardiovascular risk factors in middle-aged subjects in Taiwan. *The American Journal of the Medical Sciences*, 338(5), 268–272.

Chua B.E., Mitchell P., Wang J.J. & Rochtchina, E. (2002). Corneal Arcus and Hyperlipidemia : Findings From an Older Population. *Am J Ophthalmol.*, 363–365.

Congalton, R.G. (1991). A Review of Assessing the Accuracy of Classifications of Remotely Sensed Data. *Remote Sens. Environ*, 46, 35–46.

Cooke, N.T. (1981). Significance of arcus senilis in Caucasians. *Journal of the Royal Society of Medicine*, 74(3), 201–4.

Fernández, A., Sorokin, A. & Thompson, P.D. (2007). Corneal arcus as coronary artery disease risk factor. *Atherosclerosis*, 193(2), 235–40.

Foresee, F.D. & Hagan, M.T. (1997). Gauss-Newton Approximation to Bayesian Learning. *Network*, (7803), 4122–4128.

Halfon, S., Hames, C. & Heyden, S. (1984). Corneal arcus and coronary heart disease mortality. *Br J Ophtahlmol*, 1(X), 603–604.

Haralick, R.M., Shanmugam, K. & Dinstein, I. (1973). *Textural Features for Image Classification.* IEEE Transactions on Systems, Man and Cybernetics, SMC-3, 610–621.

Harleen, T., Harbir, S. & Ruby, B. (2014). *Eyecare Center*. Retrieved from http://www.highstreeteyecare.ca/blog/2014/2/26/the-eye-heart-connection.

Hickey, N., Maurer, B. & Mulcahy, R. (1970). Arcus senilis: its relation to certain attributes and risk factors in patients with coronary heart disease. *British Heart Journal*, 32(4), 449–52.

Hussein, S.E., Hassan, O. A. & Granat, M.H. (2013). Assessment of the potential iridology for diagnosing kidney disease using wavelet analysis and neural networks. *Biomedical Signal Processing and Control*, 8(6), 534–541.

James, I.H. (2002). *Herbal Clinic*. Retrieved from http://www.iridology-swansea.co.uk/patient-cases/patient-4/.

Keepyourhearthealthy, (2010). *Keep your heart healthy.* Retrieved from https://keepyourhearthealthy.wordpress.com/2010/05/11/arcus-senilis-its-probably-not-what-you-think/.

Kumar, A., (2008). *IIT Delhi Iris Database (version 1.0).* Retrieved from http://web.iitd.ac.in/~biometrics/Database_Iris.htm.

Lesmana, I.P.D., Purnama, I.K.E. & Purnomo, M.H. (2011). *Abnormal condition detection of pancreatic beta-cells as the cause of diabetes mellitus based on iris image*. Proceedings ICICI-BME 2011, 150–155.

Li, G. & Shi, J. (2012). Applications of Bayesian methods in wind energy conversion systems. *Renewable Energy*, 43(July 2012), 1–8.

Macchiaiolo, M., Buonuomo, P.S., Valente, P., Ran, I., Lepri, F.R, Gonfiantini, M.V. & Bartuli A. (2014). Corneal arcus as first sign of familial hypercholesterolemia. *Journal of Pediatrics*, 164(3), 670.

Navoyan, G.E. (2003). *A Case-Control Study of Corneal Arcus and Coronary Heart Disease in Yerevan*. Master of Public Health Thesis Project Utilizing Professional Publication Framework, 2013, University of Armenia.

Nor'aini A.J., Rohilah S, A.S. (2013). *Classification of Iris Regions using Principal Component Analysis and Support Vector Machine*. IEEE, 134–139.

Pomerantz, H.Z. (1962). The relationship between coronary heart disease and the presence of certain physical characteristics. *Canadian Medical Association Journal*, 86, 57–60.

Powers, D.M.W. (2007). *Evaluation: From Precision, Recall and F-Factor to ROC, Informedness, Markedness & Correlation*, Technical Report SIE-07-001, (December), 24.

Proenc, H. & Alexandre, A. (2006). *UBIRIS : A noisy iris image database.* Image Analysis and Processing – ICIAP, Volume 3617 of the Series Lecture Notes in Computer Science, 970-977.

Ramlee, R.A. & Ranjit, S. (2009). *Using Iris Recognition Algorithm, Detecting Cholesterol Presence.* International Conference on Information Management and Engineering, 714–717.

Mahesh Kumar, S.V. & Gunasundari, R. (2016). *Diagnosis of Corneal Arcus Using Statistical Feature Extraction and Support Vector Machine*. Artificial Intelligence and Evolutionary Computations in Engineering Systems, Volume 394 of the Series Advances in Intelligent Systems and Computing, 481-492.

Shannon Claude, (1948). *A Mathematical Theory of Communication.* The Bell System Technical Journal, Vol. 27, 379–423, 623–656.

Urbano, F.L., (2001). Ocular Signs of Hyperlipidemia. *Hospital Physician*, 51–54.

Wibawa, A.D. & Purnomo, M.H. (2006). *Early Detection on the Condition of Pancreas Organ as the Cause of Diabetes Mellitus by Real Time Iris Image Processing.* APCCAS 2006 - 2006 IEEE Asia Pacific Conference on Circuits and Systems, 1008–1010.

Yuan, W. & Huang, J. (2014). *Extraction and Analysis of Texture Information of the Iris Intestinal Loop.* In 9th Chinese Conference, CCBR 2014, Shenyang, China. Springer International Publishing, 328–338.

Yue, Z., Songzheng, Z. & Tianshi, L. (2011). *Bayesian Regularization BP Neural Network Model for Predicting Oil-gas Drilling Cost*. IEEE, 483–487.

Zhang, H. F., Yang, X. H., Zhao, L. D. & Wang, Y. (2009). Ultrasonic-Assisted Extraction of epimedin C from fresh leaves of Epimediumand extraction mechanism. *Innovative Food Science and Emerging Technologies*, 10(1):54–60.